



# Metalloporphyrin-based porous organic polymer as an efficient catalyst for cycloaddition of epoxides and CO<sub>2</sub><sup>☆</sup>



Ding Guo<sup>a</sup>, Cheng Li<sup>a</sup>, Juan Zhang<sup>b, \*\*</sup>, Genyan Liu<sup>a</sup>, Xiaogang Luo<sup>a, c</sup>, Fengshou Wu<sup>a, \*</sup>

<sup>a</sup> Key Laboratory of Hubei Novel Reactor and Green Chemical Technology, School of Chemical Engineering and Pharmacy, Wuhan Institute of Technology, Wuhan, 430205, PR China

<sup>b</sup> School of Chemistry and Environmental Engineering, Wuhan Institute of Technology, Wuhan, 430205, PR China

<sup>c</sup> School of Materials Science and Engineering, Zhengzhou University, Zhengzhou, 450001, PR China

## ARTICLE INFO

### Keywords:

Porous organic polymer  
Porphyrin complex  
Heterogeneous catalysis  
Carbon dioxide  
Epoxide

## ABSTRACT

The chemical fixation of carbon dioxide to afford value added chemicals under solvent free and ambient conditions has gained considerable attentions. In this work, we successfully synthesized the porphyrin-based porous organic framework (PPOPs) through Schiff base reaction using 5,10,15,20-tetra(4-aminobiphenyl) porphyrin (TAPP) and 4,4'-biphenyldicarbaldehyde (BDA) as starting materials, which was then coordinated with cobalt to yield related metal complex (Co-PPOPs). The chemical structure and morphology of Co-PPOPs were characterized by absorption spectrum, FT-IR, X-ray photoelectron spectra (XPS), scanning electron microscopy (SEM), transmission electron microscopy (TEM), X-ray powder diffraction (XRD) and nitrogen physisorption. Co-PPOPs showed excellent catalytic activity towards the conversion of carbon dioxide to cyclic carbonates under ambient conditions. Furthermore, Co-PPOPs was recovered easily and could be used repeatedly (more than five times) without losing any catalytic activity. Thus, the as-prepared Co-PPOPs was a promising heterogeneous catalyst for carbon dioxide conversion, providing high turnover number than the previously reported catalysts.

## 1. Introduction

As the main gas that causes the greenhouse effect, carbon dioxide (CO<sub>2</sub>) has the characteristics of non-toxicity, abundant, and inexpensive [1,2]. Therefore, the chemical conversion of carbon dioxide to synthesize useful intermediates for pharmaceutical or chemical industries has received considerable attentions [3–5]. Recently, the chemical fixation of CO<sub>2</sub> into epoxides to produce cyclic carbonates has drawn increasing interest due to the 100% atomic utilization rate [6]. However, because of the low reactivity of CO<sub>2</sub>, most of the reactions for the synthesis of cyclic carbonates involved harsh conditions, such as high temperature and high pressure of carbon dioxide, which limited their practical application [7].

Porous materials, including covalent organic frameworks (COF), metal organic frameworks (MOFs), and porous organic frameworks (POPs), had been widely explored in gas adsorption, storage, and sensing

due to their characteristics of high surface area, adjustable structure, and easy preparation [8–15]. Moreover, the porous materials with metal centers could be used as heterogeneous catalysts for gas capture and transformation, benefiting from their high catalytic efficiency and easy recovery [16–20]. Recently, many porous materials have been developed as efficient catalysts for the conversion of CO<sub>2</sub> into industrial raw materials, such as methanol, carbonate, and acetic acid [21–25]. However, the heterogeneous catalysts with high catalytic efficiency and stability for CO<sub>2</sub> conversion were still desirable, especially under mild reaction conditions [7].

Porphyrin and its derivatives were commonly used in photodynamic therapy due to their significant photosensitizing effect, superior photo-physical properties, and low side effects to the human body [26–29]. Because of their unique structure comprised of delocalized  $\pi$ -electrons within a tetrapyrrolic skeleton, porphyrin compounds can chelate a vast

<sup>☆</sup> Metalloporphyrin-based porous organic framework (Co-PPOPs) was prepared through Schiff base reaction, followed by the metal coordination. The chemical structure and morphology of Co-PPOPs were characterized by absorption spectrum, FT-IR, XPS, SEM, TEM, XRD, and nitrogen physisorption. Co-PPOPs displayed excellent catalytic performance for the conversion of carbon dioxide to cyclic carbonates under ambient conditions, due to the presence of porous structure and cobalt ions.

\* Corresponding author.

\*\* Corresponding author.

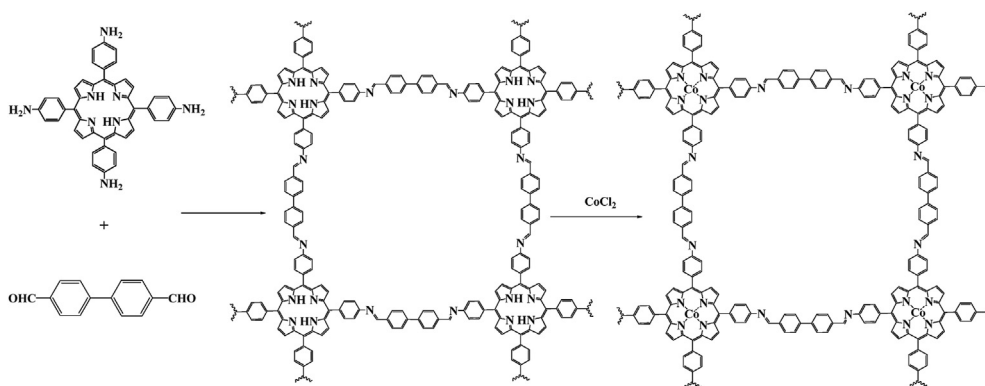
E-mail addresses: [zhang\\_juan@wit.edu.cn](mailto:zhang_juan@wit.edu.cn) (J. Zhang), [wfs42@126.com](mailto:wfs42@126.com) (F. Wu).

<https://doi.org/10.1016/j.jssc.2020.121770>

Received 28 August 2020; Received in revised form 2 October 2020; Accepted 3 October 2020

Available online xxx

0022-4596/© 2020 Elsevier Inc. All rights reserved.



**Scheme 1.** Illustration of the synthesis of Co-PPOPs by ketenimine condensation.

number of metal ions to yield related metalloporphyrin complexes [30–32]. Comparing with that of free base porphyrin, metalloporphyrin exhibits higher thermal-, chemical-, and photo-stabilities due to its larger conjugated system [20]. Furthermore, the metals in the core of porphyrin rings endowed them with potential catalytic activity. For example, the cytochrome P450 enzyme, bearing the structure of metalloporphyrin, can catalyze the conversion of alcohols to aldehydes in some organisms [33, 34].

In this context, here we synthesized a porous organic framework based on the Schiff base condensation between 5,10,15,20-tetra(4-aminophenyl)porphyrin (TAPP) and 4,4'-biphenyldicarbaldehyde (Scheme 1), which was then coordinated with cobalt to afford the related metalloporphyrin complexes (Co-PPOPs). The chemical composition and morphology of Co-PPOPs were confirmed through various characterization methods. Co-PPOPs exhibited high catalytic activity for carbon dioxide conversion to cycle carbonate under ambient conditions using a variety of substrates. Moreover, Co-PPOPs could be reused for several times without losing any significant activity, demonstrating its good recycling performance.

## 2. Experiment section

### 2.1. Materials and measurements

All chemicals were reagent-grade, purchased from Aladdin (China) and used without further purification. Scanning electron microscope (SEM) images were captured through a JEOL630-F microscope. Transmission electron microscope (TEM) images were recorded by using a JEM-3010 instrument (JEOL) equipped with slow-scan CCD camera at 300 k eV. The absorption spectra of Co-PPOPs, PPOPs and TAPP dispersed in DMSO were recorded on a UV-vis Spectrophotometer (Shimadzu). The X-ray photoelectron spectra (XPS) were carried out by Multifunctional imaging electron spectrometer (Thermo ESCALAB). The Fourier transform infrared (FT-IR) spectra were recorded by NICO-LET6700 spectrometer (ABB Bomen Canada) with KBr pellets. Powder X-ray diffraction (XRD) patterns were collected on a D8 Advance X-ray diffractometer (Bruker AXS Germany) with Cu Kr radiation at the speed of  $2^\circ \text{min}^{-1}$ . The NMR spectra of cycle carbonates were recorded on a Varian Mercury-VX 400 spectrometer in  $\text{CDCl}_3$ .

Synthesis of 5,10,15,20-tetra(4-aminophenyl) porphyrin (TAPP).

Under nitrogen atmosphere, a solution of *p*-nitrobenzaldehyde (11 g, 73 mmol) and acetic anhydride (12 mL, 127 mmol) were dissolved in 400 mL of propionic acid. After heated to  $120^\circ \text{C}$ , pyrrole (5 mL, 73 mmol) was added dropwise and the reaction solution was stirred at  $140^\circ \text{C}$  for 2 h. After cooling to room temperature, the mixture was placed in a refrigerator overnight, followed by the filtration and washing with methanol ( $100 \text{ mL} \times 3$ ) and deionized water ( $100 \text{ mL} \times 3$ ). Subsequently, the obtained black solid was recrystallized from pyridine, which was then washed with methanol/acetone (1:1) to obtain purple product (TNPP,

yield 20.5%). The TNPP (1.8 g, 2.26 mmol) was dissolved in concentrated HCl (30 mL), followed by the dropwise addition of the concentrated HCl solution (50 mL) of  $\text{SnCl}_2$  (7.0 g, 29 mol). The reaction solution was stirred at room temperature for 2 h, and then heated to  $80^\circ \text{C}$  for 0.5 h under nitrogen atmosphere. After the completion of reaction, the mixture was cooled to  $0^\circ \text{C}$ , and neutralized with ammonia water. The purple product was obtained by filtering and Soxhlet extraction with chloroform (yield 80%).  $^1\text{H NMR}$  (400 MHz,  $\text{CDCl}_3$ )  $\delta$  8.90 (s, 8H), 7.99 (d,  $J = 8.2 \text{ Hz}$ , 8H), 7.07 (d,  $J = 8.2 \text{ Hz}$ , 8H), 4.03 (s, 8H),  $-2.71$  (s, 2H). MALDI-TOF-MS spectrum of TAPP, calcd for  $\text{C}_{44}\text{H}_{34}\text{N}_8$ : 674.3122; Found: 674.3034.

### 2.2. Synthesis of PPOPs

A Pyrex tube (12 mL) was charged with TAPP (200 mg, 0.26 mmol), 4,4'-biphenyldicarbaldehyde (55 mg, 0.52 mmol), 1,2-dichlorobenzene (4 mL), *n*-butanol (4 mL) and 6 M aqueous acetic acid (0.5 mL). After sonication for 15 min, the tube was frozen under liquid nitrogen bath, evacuated and flame sealed. The reaction mixture was then heated at  $120^\circ \text{C}$  for 72 h to afford a reddish-brown precipitate, which was then purified through Soxhlet extraction using anhydrous THF with solvent (yield 75%).

### 2.3. Synthesis of Co-PPOPs

A solution of  $\text{CoCl}_2 \cdot 6\text{H}_2\text{O}$  (200 mg 0.84 mmol) in *N*-Methyl pyrrolidone (NMP) (15 mL) was added to a glass flask containing PPOPs (100 mg). After stirring at  $80^\circ \text{C}$  for 48 h, the solution was filtered and the obtained solid was washed repeatedly with dichloromethane ( $50 \text{ mL} \times 3$ ) and chloroform ( $50 \text{ mL} \times 3$ ), respectively. The product was recrystallized from methanol and then dried under vacuum to afford Co-PPOPs as a black solid (yield 90%).

### 2.4. Catalytic test

The catalytic performances of Co-PPOPs were evaluated using various substrates, such as styrene oxide, 2-(chloromethyl) oxirane, 2-(bromo-methyl) oxirane and so on. Using styrene oxide as a representative substrate, the catalytic reaction was carried out at room temperature in a 25 mL Schlenk flask. In general, a mixture of tetrabutyl ammonium bromide (TBAB, 0.58 g, 1.8 mmol), Co-PPOPs (20 mg) and styrene oxide (3.00 g, 25 mmol) was successively added to the flask.  $\text{CO}_2$  at atmospheric pressure was then injected through a gas bag. After stirring at room temperature for 48 h, the reaction mixture was centrifuged and the insoluble solid were washed with methanol and dichloromethane for several times. The product yield was determined by gas chromatography (GC) using chlorobenzene as an internal standard. Further purification of the crude product was carried out by silica gel column chromatography to obtain the pure styrene carbonate for NMR characterization.

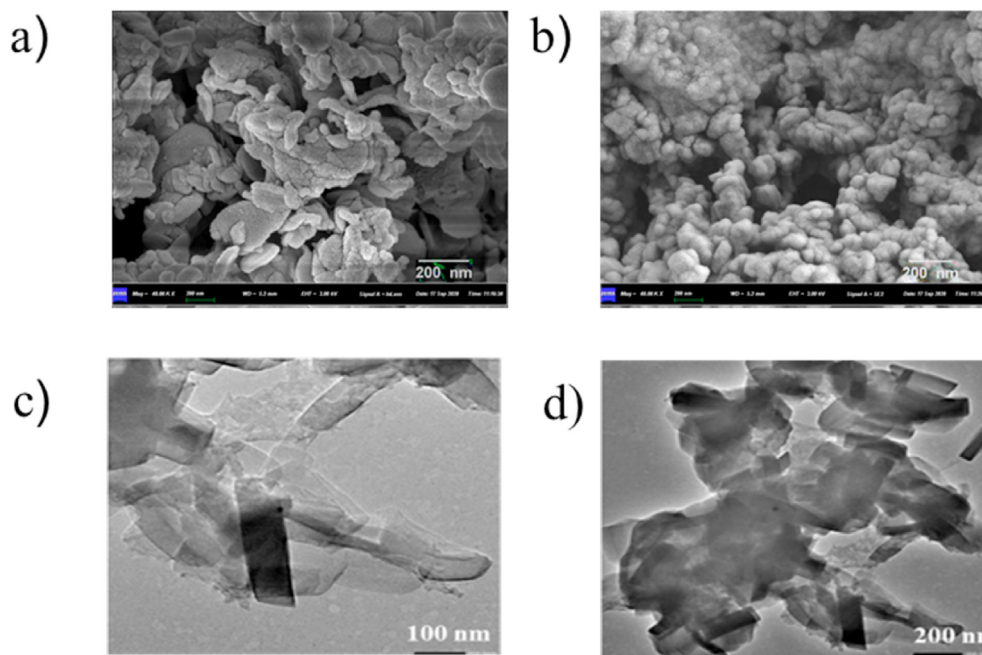


Fig. 1. SEM images of (a) PPOPs, (b) Co-PPOPs, and TEM images of (c) PPOPs, (d) Co-PPOPs.

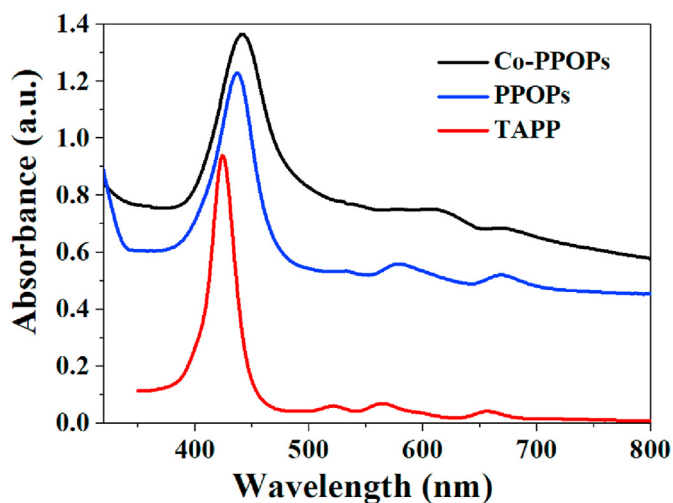


Fig. 2. The UV-vis absorption spectrum of Co-PPOPs (black), PPOPs (blue) and TAPP (red), dispersed in DMSO. (For interpretation of the references to colour in this figure legend, the reader is referred to the Web version of this article.)

### 3. Results and discussion

#### 3.1. Structural and morphological characterization

The synthetic routes of Co-PPOPs were outlined in Scheme 1. Under solvothermal conditions, TAPP was reacted with BDA to afford PPOPs, which was then coordinated with  $\text{CoCl}_2 \cdot 6\text{H}_2\text{O}$  to afford Co-PPOP with high yield. Both of PPOPs and Co-PPOPs were insoluble in water and common organic solvents, such as methanol, dichloromethane, petroleum ether, tetrahydrofuran, and *N,N*-dimethylformamide. The X-ray powder diffraction (XRD) patterns of Co-PPOPs exhibited a broad diffraction peak centered around  $22^\circ$  (Fig. S1), revealing the amorphous nature of porous structure. The functional groups of Co-PPOPs and PPOPs were confirmed by FT-IR spectra. As shown in Fig. S2, both of Co-PPOPs and PPOPs exhibited the apparent peak at  $1602\text{ cm}^{-1}$ , which could be ascribed to the characteristic  $\text{C}=\text{N}$  stretching. Moreover, the  $-\text{CHO}$

stretching bands ( $1688\text{ cm}^{-1}$ ) of BDA disappeared in Co-PPOPs, indicating the success of ketenimine condensation.

The thermal behavior of PPOPs and Co-PPOPs was studied by thermogravimetric analysis (TGA) under continuous flow of nitrogen gas. As shown in Fig. S3, PPOPs and Co-PPOPs displayed the high thermal stability with the decomposition temperature up to  $300^\circ\text{C}$ . The morphology and porosity of PPOPs and Co-PPOPs were characterized through scanning electron microscope (SEM) and transmission electron microscope (TEM). Fig. 1a and Fig. 1b showed the SEM images of PPOPs and Co-PPOPs respectively, giving direct evidence for the presence of porous structures due to their highly crosslinked backbones. The TEM images of PPOPs and Co-PPOPs exhibited the typical lamellar structure with regular shape as indicated in Fig. 1c and d. Moreover, the UV-vis spectrum of both TAPP and Co-PPOPs exhibited characteristic Soret peak ( $425\text{ nm}$ ) and Q bands ( $500\text{--}700\text{ nm}$ ), indicating the presence of porphyrin ring. Comparing with that of TAPP, the Soret peak of Co-PPOPs and PPOPs redshifted to some extent, probably ascribed to the increase of conjugation in porous organic polymer (Fig. 2).

The chemical composition of PPOPs and Co-PPOPs was characterized by X-ray photoelectron spectroscopy (XPS). The elementary composition of PPOPs was confirmed by XPS spectrum (Fig. S4), from which the content of C and N was calculated to be 81.56% and 9.87%, respectively. These values were consistent with that of theoretical values (C, 85.27%; N, 10.29%) of PPOPs. The high-resolution N1s XPS spectrum of Co-PPOPs showed two peaks at 399.3, 398.9 eV and 400.4 eV (Fig. 3), assigned to pyridinic nitrogen and free amine ( $-\text{C}=\text{N}$ ), respectively. Compared with the XPS of PPOPs (Fig. S4), the asymmetric broad peak at 780.7 eV was observed in Co-PPOPs, corresponding to the characteristic  $\text{CoN}_4$  center [7]. Moreover, the weak peaks at 288 eV in high resolution of C1s spectrum and 406 eV in high resolution of N 1s spectrum were probably caused by the background signal. Energy-dispersive X-ray spectroscopy (EDS) of Co-PPOPs also verified the presence of Co element (Fig. 4), indicating the successful coordination of cobalt ions in the core of PPOPs. The cobalt content of Co-PPOPs was calculated to be 0.72 wt% through the atoms absorption spectroscopy (AAS). Thus, not all the porphyrin macrocycle in the porous organic polymer was chelated with cobalt. The reason for this result was probably ascribed to the poor solubility of PPOPs in the general organic solvents. Thus, the heterogeneous reaction between PPOPs and  $\text{CoCl}_2 \cdot 6\text{H}_2\text{O}$  in *N*-Methyl pyrrolidone

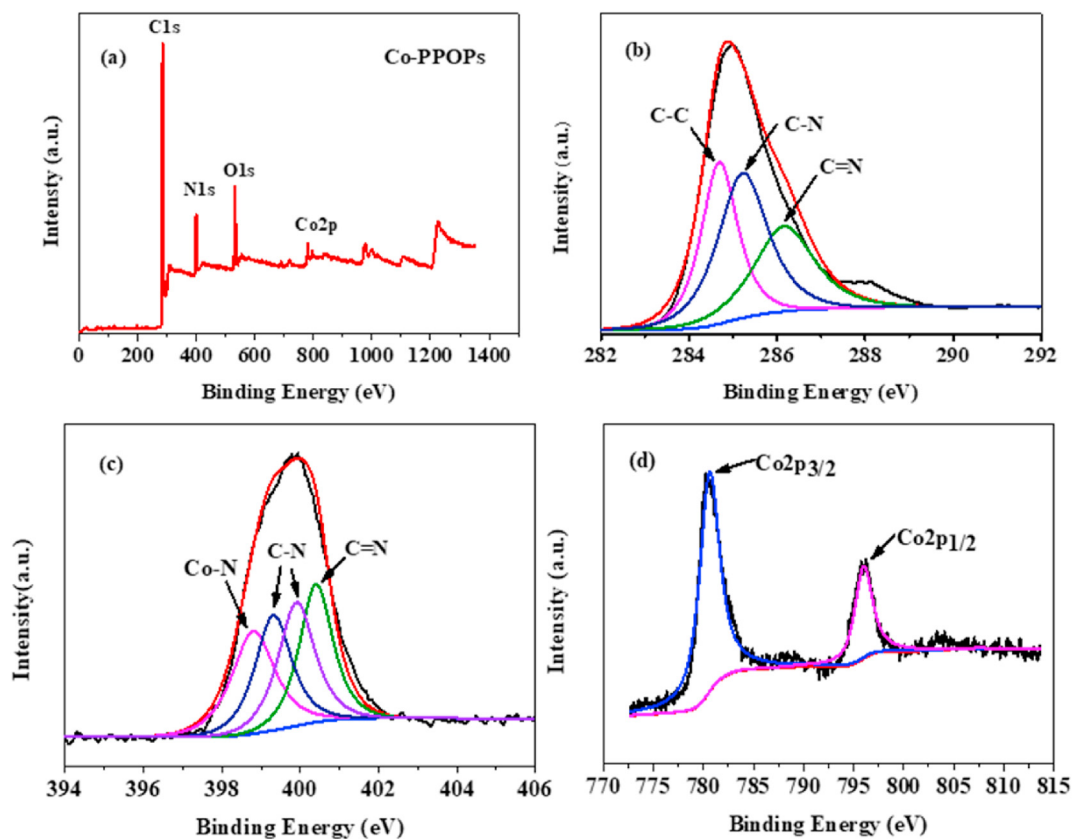


Fig. 3. XPS spectra for Co-PPOPs (a), C1s of Co-PPOPs (b), N1s of Co-PPOPs (c) and Co2p of Co-PPOPs (d).

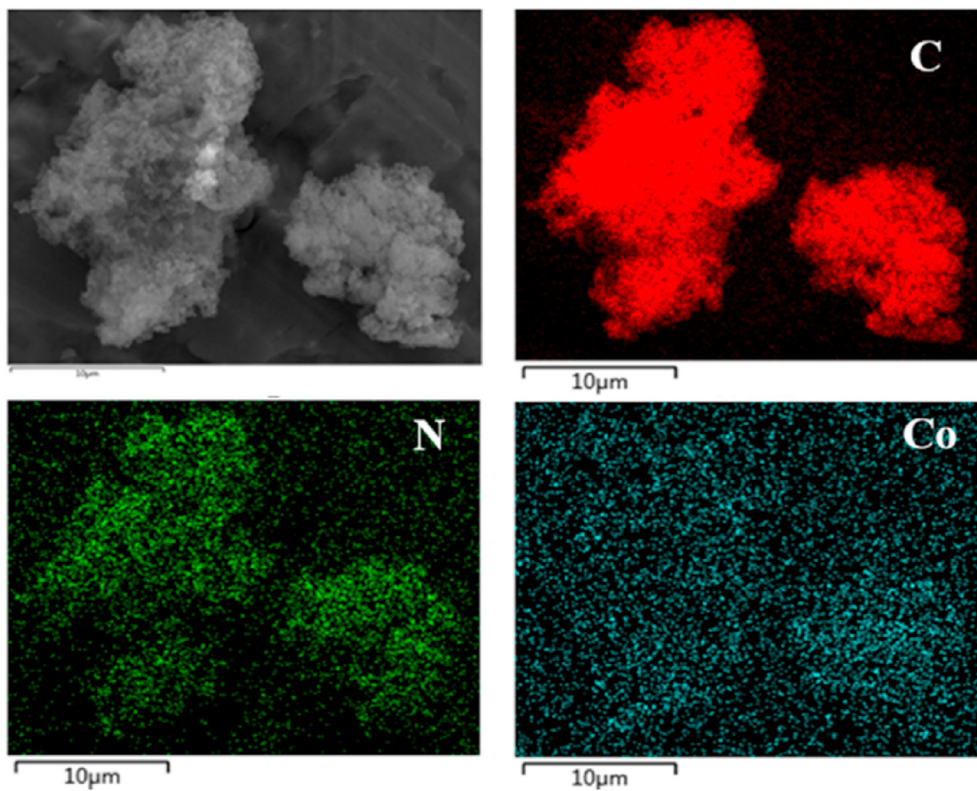


Fig. 4. Electron image and element mapping (C, N, Co) spectra of Co-PPOPs.



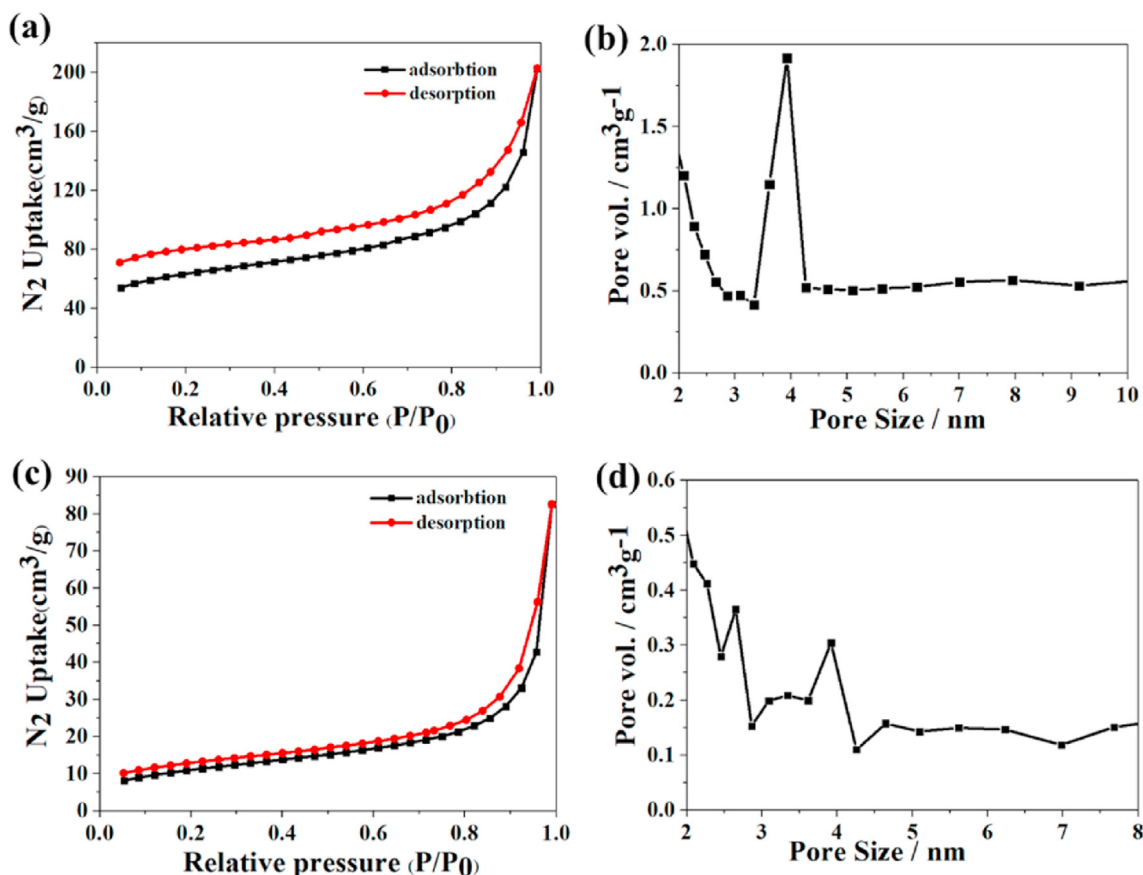


Fig. 5.  $N_2$  adsorption isotherms of PPOPs (a) and Co-PPOPs (c) at 77 K; Pore size distributions of PPOPs (b) and Co-PPOPs (d).

**Table 1**  
Coupling of  $CO_2$  and styrene oxide catalyzed by different catalytic system<sup>a</sup>.

Entry	Catalyst	TBAB	Yield (%) <sup>b</sup>	TON
1	None	None	0	–
2	Co-PPOPs	None	3	313
3	None	1.8 mmol	22	–
4	PPOPs	1.8 mmol	21	2188
5	Co-PPOPs	1.8 mmol	98	10,208

<sup>a</sup> Typical reaction conditions: a reactor with a 25 mL Schlenk flask; 25 mmol styrene oxide with 20 mg catalyst,  $CO_2$  pressure (1 atm); room temperature; reaction time (48 h).

<sup>b</sup> Yields determined by GC using chlorobenzene as internal standard.

(NMP) would result in the low reaction efficiency. The reaction efficiency might be improved by prolonging the reaction time.

Nitrogen adsorption-desorption isotherms of porous organic polymers were shown in Fig. 5. Both of PPOPs and Co-PPOPs displayed type I patterns with a sharp uptake under the low relative pressure region ( $P/P_0 < 0.1$ ), which were reasonably associated with the presence of mesopores and micropores. The Brunauer-Emmett-Teller surface area of PPOPs and Co-PPOPs were calculated to be 226  $m^2/g$  and 39  $m^2/g$ ,

**Table 2**

The catalytic performance for chemical conversion of  $CO_2$  into styrene carbonate catalyzed by various catalytic systems.

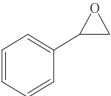
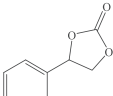
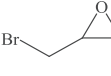
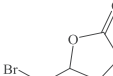
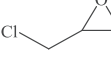
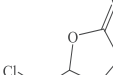
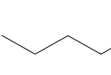
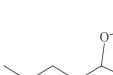
Entry	Catalyst	Active center	T (°C)	P (MPa)	Time (h)	Yield (%)	TON	Ref.
1	Co-PPOPs	Co	25	0.1	48	98	10,208	This work
2	HUST-1-Co	Co	25	0.1	48	93.2	2760	[7]
3	Al-iPOP-1	Al	25	0.1	9	52	156	[20]
4	COF-HNU3	Imidazolium Salt	100	2	72	94	470,000	[22]
5	2,3-DhaTph	Hydroxyl	110	1	12	98	490	[35]
6	TBA-TBD-P	Phosphonate Salt	80	0.1	10	69.6	214	[36]

respectively. The DFT fitting of the adsorption branches suggested the pore size was mainly around 4 nm (Fig. 3c and d), which were consistent with the shape of nitrogen adsorption isotherms and SEM analysis.

### 3.2. Catalytic properties

With Co-PPOPs in hand, its ability to catalyze the cycloaddition of epoxides and  $CO_2$  to synthesize the cyclic carbonates was examined. As shown in Table 1, Co-PPOPs showed excellent catalytic activity in the cycloaddition of  $CO_2$  with styrene oxide (SO) under ambient conditions. no product was detected without the addition of catalyst and TBAB (Table 1, entry 1). The yield of styrene carbonate (SC) was only 3% when catalyzed by bare Co-PPOPs (Table 1, entry 2), even extending the reaction time. Besides, only 22% yield was obtained when bare TBAB was used (Table 1, entry 3). Moreover, the yield catalyzed by PPOPs and TBAB was also only 21% after 48 h (Table 1, entry 4), indicating the negligible catalytic activity of Co-free PPOPs. In contrast, the yield of SC was promoted to 98% when the combined catalysts of Co-PPOPs and TBAB was used (Table 1, entry 5). The high catalytic activity of Co-PPOPs was probably derived from the cooperative effect of metal center (Co) and nucleophilic halide anion ( $X^-$ ) in TBAB. Compared with other

**Table 3**  
Synthesis of various cyclic carbonates using Co-PPOPs as catalyst<sup>a</sup>.

Entry	Epoxides	Products	Time (h)	Yields (%) <sup>b</sup>	TON
1			48	98	10,208
2			36	96 <sup>c</sup>	10,000
3			36	97	10,104
4			36	92	9583

<sup>a</sup> Reaction conditions: epoxide (25 mmol), Co-PPOPs (20 mg), TBAB (n-Bu<sub>4</sub>NBr, 1.8 mmol), room temperature under CO<sub>2</sub>.

<sup>b</sup> Yields determined by GC using chlorobenzene as internal standard.

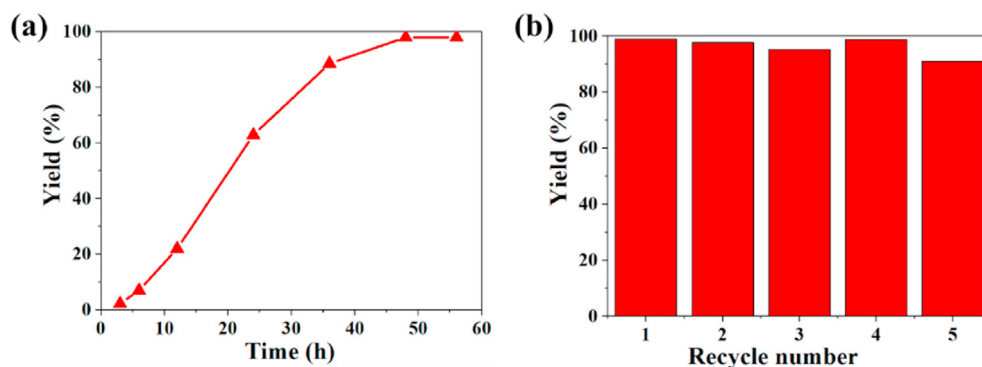
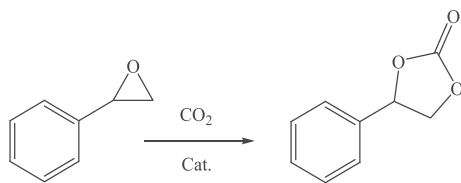


**Fig. 6.** Yield of styrene carbonate catalyzed by Co-PPOPs (a); the recyclability of Co-PPOPs (b).

reported catalysts with different active center, Co-PPOPs exhibited a higher catalytic efficiency in the cycloaddition of epoxides and CO<sub>2</sub>, as shown in Table 2. Although COF-HNU3 had a higher TON value (Table 2, entry 4), the reaction required higher temperature (100 °C) and carbon dioxide pressure (2 MPa), and longer reaction time (72 h) [19]. The yield of cyclic carbonate catalyzed by 2,3-DhaTph also reached 98%. However, the reaction temperature needed to be raised above 110 °C [32]. Since Co-PPOPs exhibited high TON and catalytic yields under ambient conditions, it was superior in terms of reaction temperature, CO<sub>2</sub> pressure and reaction time.

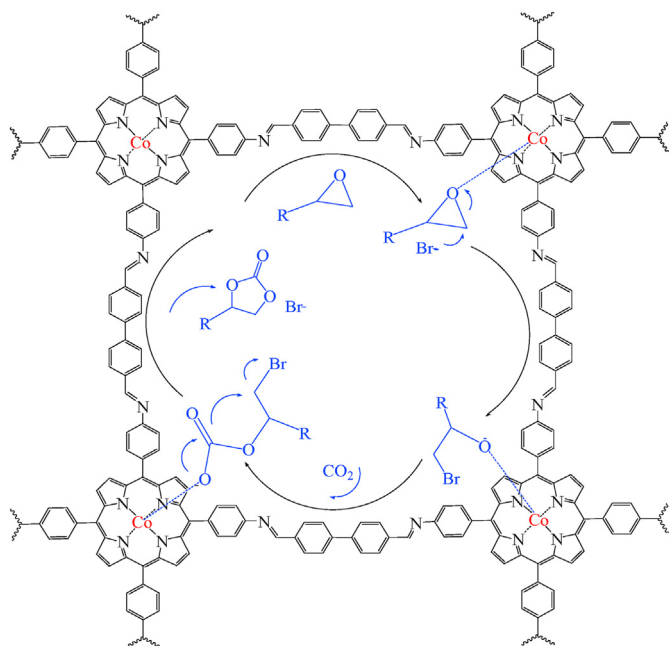


Generally, a catalyst showed different activity for different substrates. Therefore, after establishing the high catalytic activity of Co-PPOPs for styrene carbonate formation, a variety of substrates were further evaluated under room temperature. As shown in Table 3, the yield of styrene carbonate (98%) was highest among these substrates, and the related TON (turnover number) was calculated to be 10,208. In contrast, 1,2-epoxyhexane displayed the lowest yield when catalyzed by Co-PPOPs. These results indicated that the electron-withdrawing substituents in epoxy compound could activate the cycloaddition process to some extent. The structure of various styrene carbonates was confirmed by NMR

spectrum (Figs. S7–S10).

Although reaction yields at long times are useful information for synthetic purposes, to assess the utility of the catalyst, it is best to gather kinetic profiles for the reactions. To this end, the kinetic experiments were performed for the cycloaddition of styrene with CO<sub>2</sub>, as shown in Fig. 6a. The kinetic profiles revealed the high reaction rate at the early stage, with initial TOF (turnover frequency) about 121.5 h<sup>-1</sup>. After 48 h, the yield of styrene carbonate reached 98%, and no appreciable change in the yield of the product was found with the extension of reaction time. Considering the heterogeneous nature of the synthesized polymeric catalysts, the recyclability and reusability of Co-PPOPs were assessed by performing styrene/CO<sub>2</sub> cycloaddition under ambient conditions. After each run, the insoluble catalyst can be easily recovered by simply washing and drying, and reused directly for the next cycle. As shown in Fig. 6b, Co-PPOPs can be recycled for at least five successive times without any significant decrease in catalytic activity, and the yield of product remained over 98% during each cycle, indicating the good recycling performance. After three times recycle, the EDS and XPS spectrum of recovered Co-PPOPs were measured. As shown in Fig. S5 and Fig. S6, no obvious variation of chemical composition was found before and after the catalyst was used, indicating the high stability of Co-PPOPs.

Based on the previous reports on the catalytic formation of carbonates from CO<sub>2</sub> [35–38], a tentative mechanism of Co-PPOPs was demonstrated. As shown in Scheme 2, the high activity of the catalyst was probably derived from the cooperative effect of Lewis acid metal center (Co) and porous reticular structure of Co-PPOPs. Specifically, the oxygen atom of the epoxide firstly combined with the metal center of Co-PPOPs through electrostatic interaction to form the Co–O bond. The



**Scheme 2.** Proposed reaction mechanism for the synthesis of cyclic carbon dioxide and epoxide with Co-PPOPs as a catalyst.

nucleophilic addition reaction then occurred via halogen (Br) attack, resulting in the ring opening of substrate. Subsequently, the enriched CO<sub>2</sub> around the cobalt center inserted quickly into the Co–O bond of opened epoxy to form an intermediate. With the departure of halogen and the desorption of the intermediate from Co-PPOPs, the corresponding cyclic carbonate was obtained. Meanwhile, the catalyst was recovered and could work in the next cycle.

#### 4. Conclusions

In summary, a metalloporphyrin-based porous organic polymer (Co-PPOPs) was prepared through Schiff base reaction, followed by the incorporation of Co ion. Co-PPOPs exhibited high catalytic efficiency for the cycloaddition of various epoxides with CO<sub>2</sub>. The TON value for the synthesis of styrene carbonate was as high as 10,208 at room temperature and atmospheric pressure. The high catalytic activity was probably derived from the cooperative effect of Lewis acid metal center (Co) and porous reticular structure of Co-PPOPs. More importantly, Co-PPOPs can be recycled for at least five successive times without any significant decrease in catalytic activity, and the yield of product remained over 98% during each cycle, indicating the good recycling performance. These results could inspire more environmentally catalysts for fixation of carbon dioxide to yield valuable products at ambient conditions.

#### CRediT authorship contribution statement

**Ding Guo:** Methodology, Investigation, Formal analysis, Data curation, Writing - original draft, Writing - review & editing. **Cheng Li:** Conceptualization, Methodology, Data curation. **Juan Zhang:** Conceptualization, Writing - review & editing, Funding acquisition. **Genyan Liu:** Formal analysis, Methodology, Data curation. **Xiaogang Luo:** Formal analysis, Methodology, Data curation. **Fengshou Wu:** Conceptualization, Supervision, Funding acquisition, Writing - review & editing.

#### Declaration of competing interest

The authors declare that they have no known competing financial interests or personal relationships that could have appeared to influence the work reported in this paper.

#### Acknowledgements

This work was supported by the National Natural Science Foundation of China (NSFC) (grant no. 21601142, 81503036), Key Project of Scientific Research Project of Hubei Provincial Department of Education (grant no. D20201504), and Outstanding Young and Middle-aged Scientific Innovation Team of Colleges and Universities of Hubei Province: “Biomass chemical technologies and materials” (grant no. T201908).

#### Appendix A. Supplementary data

Supplementary data to this article can be found online at <https://doi.org/10.1016/j.jssc.2020.121770>.

#### Declaration of interest statement

All authors declare no potential conflict of interest.

#### Data availability

All the data pertaining to this study is included in the main article and supplementary material. The raw/processed data is available from the corresponding author upon reasonable request.

#### References

- [1] D.J. Darensbourg, A.D. Yeung, A concise review of computational studies of the carbon dioxide–epoxide copolymerization reactions, *Polym. Chem.* 5 (13) (2014) 3949–3962.
- [2] S. Liu, F. Chen, S. Li, X. Peng, Y. Xiong, Enhanced photocatalytic conversion of greenhouse gas CO<sub>2</sub> into solar fuels over g-C<sub>3</sub>N<sub>4</sub> nanotubes with decorated transparent ZIF-8 nanoclusters, *Appl. Catal. B Environ.* 211 (2017) 1–10.
- [3] T. Ishida, S. Kikuchi, T. Tsubo, T. Yamada, Silver-catalyzed incorporation of carbon dioxide into o-alkynylaniline derivatives, *Org. Lett.* 15 (4) (2013) 848–851.
- [4] A. Berkefeld, W.E. Piers, M. Parvez, L. Castro, L. Maron, O. Eisenstein, Decamethylscandocinium-hydroxo-(perfluorophenyl)borate: fixation and tandem tris(perfluorophenyl)borane catalyzed deoxygenative hydrosilylation of carbon dioxide, *Chem. Sci.* 4 (5) (2013) 2152–2162.
- [5] H. Mizuno, J. Takaya, N. Iwasawa, Rhodium(I)-catalyzed direct carboxylation of arenes with CO<sub>2</sub> via chelation-assisted C–H bond activation, *J. Am. Chem. Soc.* 133 (5) (2011) 1251–1253.
- [6] C. Federsel, A. Boddien, R. Jackstell, R. Jennerjahn, P.J. Dyson, R. Scopelliti, G. Laurenczy, M. Beller, A well-defined iron catalyst for the reduction of bicarbonates and carbon dioxide to formates, alkyl formates, and formamides, *Angew. Chem. Int. Ed.* 49 (50) (2010) 9777–9780.
- [7] S. Wang, K. Song, C. Zhang, Y. Shu, T. Li, B. Tan, A novel metalloporphyrin-based microporous organic polymer with high CO<sub>2</sub> uptake and efficient chemical conversion of CO<sub>2</sub> under ambient conditions, *J. Mater. Chem.* 5 (4) (2017) 1509–1515.
- [8] J. Huang, S.R. Turner, Hypercrosslinked polymers: a review, *Polym. Rev.* 58 (1) (2017) 1–41.
- [9] P.M. Budd, A. Butler, J. Selbie, K. Mahmood, N.B. McKeown, B. Ghanem, K. Msayib, D. Book, A. Walton, The potential of organic polymer-based hydrogen storage materials, *Phys. Chem. Chem. Phys.* 9 (15) (2007) 1802–1808.
- [10] N. Huang, P. Wang, D. Jiang, Covalent organic frameworks: a materials platform for structural and functional designs, *Nat. Rev. Mater.* 1 (10) (2016) 16068.
- [11] Y. Xu, S. Jin, H. Xu, A. Nagai, D. Jiang, Conjugated microporous polymers: design, synthesis and application, *Chem. Soc. Rev.* 42 (20) (2013) 8012–8031.
- [12] L. Tan, B. Tan, Hypercrosslinked porous polymer materials: design, synthesis, and applications, *Chem. Soc. Rev.* 46 (11) (2017) 3322–3356.
- [13] P. Li, F.-F. Cheng, W.-W. Xiong, Q. Zhang, New synthetic strategies to prepare metal-organic frameworks, *Inorg. Chem. Front.* 5 (11) (2018) 2693–2708.
- [14] F.-F. Cheng, J.-N. Zhu, M.-Y. Zhao, Z.-J. Ma, W.-W. Xiong, Preparing transition metal-organic frameworks based on oxalate-sulfate anions in deep eutectic solvents, *J. Solid State Chem.* 278 (2019) 120904.
- [15] W.W. Xiong, Q. Zhang, Surfactants as promising media for the preparation of crystalline inorganic materials, *Angew. Chem. Int. Ed.* 54 (40) (2015) 11616–11623.
- [16] R.R. Haikal, A.B. Soliman, M. Amin, S.G. Karakalos, Y.S. Hassan, A.M. Elmansi, I.H. Hafez, M.R. Berber, A. Hassani, M.H. Alkordi, Synergism of carbon nanotubes and porous-organic polymers (POPs) in CO<sub>2</sub> fixation: one-pot approach for bottom-up assembly of tunable heterogeneous catalyst, *Appl. Catal. B Environ.* 207 (2017) 347–357.
- [17] S.K. Dey, D. Dietrich, S. Wegner, B. Gil-Hernández, S.S. Harmalkar, N. deSousaAmadeu, C. Janiak, Palladium nanoparticle-immobilized porous polyurethane material for quick and efficient heterogeneous catalysis of suzuki-miyaura cross-coupling reaction at room temperature, *Chemistry* 3 (5) (2018) 1365–1370.

- [18] H. Zhong, Y. Su, X. Chen, X. Li, R. Wang, Imidazolium- and triazine-based porous organic polymers for heterogeneous catalytic conversion of CO<sub>2</sub> into cyclic carbonates, *ChemSusChem* 10 (24) (2017) 4855–4863.
- [19] W.M. Liao, J.H. Zhang, Z. Wang, Y.L. Lu, S.Y. Yin, H.P. Wang, Y.N. Fan, M. Pan, C.Y. Su, Semiconductive amine-functionalized Co(II)-MOF for visible-light-driven hydrogen evolution and CO<sub>2</sub> reduction, *Inorg. Chem.* 57 (18) (2018) 11436–11442.
- [20] Y. Chen, R. Luo, Q. Xu, J. Jiang, X. Zhou, H. Ji, Charged metalloporphyrin polymers for cooperative synthesis of cyclic carbonates from CO<sub>2</sub> under ambient conditions, *ChemSusChem* 10 (11) (2017) 2534–2541.
- [21] B. An, L. Zeng, M. Jia, Z. Li, Z. Lin, Y. Song, Y. Zhou, J. Cheng, C. Wang, W. Lin, Molecular iridium complexes in metal-organic frameworks catalyze CO<sub>2</sub> hydrogenation via concerted proton and hydride transfer, *J. Am. Chem. Soc.* 139 (49) (2017) 17747–17750.
- [22] J. Qiu, Y. Zhao, Z. Li, H. Wang, Y. Shi, J. Wang, Imidazolium-salt-Functionalized covalent organic frameworks for highly efficient catalysis of CO<sub>2</sub> conversion, *ChemSusChem* 12 (11) (2019) 2421–2427.
- [23] X. Deng, J. Albero, L. Xu, H. Garcia, Z. Li, Construction of a stable Ru-Re hybrid system based on multifunctional MOF-253 for efficient photocatalytic CO<sub>2</sub> reduction, *Inorg. Chem.* 57 (14) (2018) 8276–8286.
- [24] Y. Fu, D. Sun, Y. Chen, R. Huang, Z. Ding, X. Fu, Z. Li, An amine-functionalized titanium metal-organic framework photocatalyst with visible-light-induced activity for CO<sub>2</sub> reduction, *Angew. Chem. Int. Ed.* 51 (14) (2012) 3364–3367.
- [25] W. Liang, T.L. Church, S. Zheng, C. Zhou, B.S. Haynes, D.M. D'Alessandro, Site isolation leads to stable photocatalytic reduction of CO<sub>2</sub> over a rhenium-based catalyst, *Chem. Eur. J.* 21 (51) (2015) 18576–18579.
- [26] M. Yang, S. Cao, X. Sun, H. Su, H. Li, G. Liu, X. Luo, F. Wu, Self-assembled naphthalimide conjugated porphyrin nanomaterials with D-A structure for PDT/PTT synergistic therapy, *Bioconjugate Chem.* 31 (3) (2020) 663–672.
- [27] L. Yang, H. Li, D. Liu, H. Su, K. Wang, G. Liu, X. Luo, F. Wu, Organic small molecular nanoparticles based on self-assembly of amphiphilic fluoroporphyrins for photodynamic and photothermal synergistic cancer therapy, *Colloids Surf., B* 182 (2019) 110345.
- [28] F. Wu, L. Chen, L. Yue, K. Wang, K. Cheng, J. Chen, X. Luo, T. Zhang, Small-molecule porphyrin-based organic nanoparticles with remarkable photothermal conversion efficiency for in vivo photoacoustic imaging and photothermal therapy, *ACS Appl. Mater. Interfaces* 11 (24) (2019) 21408–21416.
- [29] F. Wu, J. Chen, Z. Li, H. Su, K.C.-F. Leung, H. Wang, X. Zhu, Red/near-infrared emissive metalloporphyrin-based nanodots for magnetic resonance imaging-guided photodynamic therapy in vivo, *Part. Part. Syst. Char.* 35 (9) (2018) 1800208.
- [30] M. Yang, J. Deng, D. Guo, J. Zhang, L. Yang, F. Wu, A folate-conjugated platinum porphyrin complex as a new cancer-targeting photosensitizer for photodynamic therapy, *Org. Biomol. Chem.* 17 (21) (2019) 5367–5374.
- [31] M. Yang, J. Deng, D. Guo, Q. Sun, Z. Wang, K. Wang, F. Wu, Mitochondria-targeting Pt/Mn porphyrins as efficient photosensitizers for magnetic resonance imaging and photodynamic therapy, *Dyes Pigments* 166 (2019) 189–195.
- [32] F. Wu, M. Yang, J. Zhang, S. Zhu, M. Shi, K. Wang, Metalloporphyrin-indomethacin conjugates as new photosensitizers for photodynamic therapy, *J. Biol. Inorg. Chem.* 24 (1) (2019) 53–60.
- [33] M. Gao, F. Yu, C. Lv, J. Choo, L. Chen, Fluorescent chemical probes for accurate tumor diagnosis and targeting therapy, *Chem. Soc. Rev.* 46 (8) (2017) 2237–2271.
- [34] H. Chen, Z. Gu, H. An, C. Chen, J. Chen, R. Cui, S. Chen, W. Chen, X. Chen, X. Chen, Z. Chen, B. Ding, Q. Dong, Q. Fan, T. Fu, D. Hou, Q. Jiang, H. Ke, X. Jiang, G. Liu, S. Li, T. Li, Z. Liu, G. Nie, M. Ovais, D. Pang, N. Qiu, Y. Shen, H. Tian, C. Wang, H. Wang, Z. Wang, H. Xu, J.-F. Xu, X. Yang, S. Zhu, X. Zheng, X. Zhang, Y. Zhao, W. Tan, X. Zhang, Y. Zhao, Precise nanomedicine for intelligent therapy of cancer, *Sci. China Chem.* 61 (12) (2018) 1503–1552.
- [35] V. Saptal, D.B. Shinde, R. Banerjee, B.M. Bhanage, State-of-the-art catechol porphyrin COF catalyst for chemical fixation of carbon dioxide via cyclic carbonates and oxazolidinones, *Catal. Technol.* 6 (15) (2016) 6152–6158.
- [36] J. Fang, K. Li, Z. Wang, D. Li, Y. Ma, X. Gong, Z. Hou, Direct oxidative carboxylation of olefins into cyclic carbonates at ambient pressure, *J. CO<sub>2</sub> Util.* 40 (2020) 101204.
- [37] T. Ema, Y. Miyazaki, J. Shimonishi, C. Maeda, J.Y. Hasegawa, Bifunctional porphyrin catalysts for the synthesis of cyclic carbonates from epoxides and CO<sub>2</sub>: structural optimization and mechanistic study, *J. Am. Chem. Soc.* 136 (43) (2014) 15270–15279.
- [38] Z. Guo, X. Cai, J. Xie, X. Wang, Y. Zhou, J. Wang, Hydroxyl-exchanged nanoporous ionic copolymer toward low-temperature cycloaddition of atmospheric carbon dioxide into carbonates, *ACS Appl. Mater. Interfaces* 8 (20) (2016) 12812–12821.